How to cite: *Angew. Chem. Int. Ed.* **2023**, *62*, e202310989
doi.org/10.1002/anie.202310989

Recyclable Polymers | Hot Paper

Highly Recyclable and Tough Elastic Vitrimers from a Defined Polydimethylsiloxane Network

Jiancheng Luo, Xiao Zhao, Hao Ju, Xiangjun Chen, Sheng Zhao, Zoriana Demchuk, Bingrui Li, Vera Bocharova, Jan-Michael Y. Carrillo, Jong K. Keum, Sheng Xu, Alexei P. Sokolov, Jiayao Chen, and Peng-Fei Cao**

Abstract: Despite intensive research on sustainable elastomers, achieving elastic vitrimers with significantly improved mechanical properties and recyclability remains a scientific challenge. Herein, inspired by the classical elasticity theory, we present a design principle for ultra-tough and highly recyclable elastic vitrimers with a defined network constructed by chemically crosslinking the pre-synthesized disulfide-containing polydimethylsiloxane (PDMS) chains with tetra-arm polyethylene glycol (PEG). The defined network is achieved by the reduced dangling short chains and the relatively uniform molecular weight of network strands. Such elastic vitrimers with the defined network, i.e., PDMS-disulfide-D, exhibit significantly improved mechanical performance than random analogous, previously reported PDMS vitrimers, and even commercial silicone-based thermosets. Moreover, unlike the vitrimers with random network that show obvious loss in mechanical properties after recycling, those with the defined network enable excellent thermal recyclability. The PDMS-disulfide-D also deliver comparable electrochemical signals if utilized as substrates for electromyography sensors after the recycling. The multiple relaxation processes are revealed via a unique physical approach. Multiple techniques are also applied to unravel the microscopic mechanism of the excellent mechanical performance and recyclability of such defined network.

Introduction

For centuries, elastomers have been widely used in numerous traditional applications, such as tires, sealants, footwear, wire coatings, and automotive manufacturing.[1] Recently, they also enable the rapid development of stretchable devices/electronics, wearable sensors, and soft robotics.[2] Therefore, designing elastomers with superior properties such as mechanical robustness, excellent chemical and heat resistance, high stretchability and excellent re-processability, *etc.*, has always been attractive for different applications. However, these properties are usually difficult to improve simultaneously because they exhibit a trade-off behavior.[3] For example, thermoplastic elastomers show excellent stretchability and re-processability while having a low tolerance to heat and chemicals. On the other hand, thermoset elastomers are good candidates for application fields requiring high thermal and chemical stability, however, they are difficult to be malleable or recycled due to the presence of permanent chemical crosslinks. Fortunately, the significant progress in dynamic covalent networks (DCNs) serves as a "catalyst" to overcome this barrier.[4] Instead of permeant chemical crosslinks, DCNs contain dynamic covalent bonds that can undergo either dissociative or associative exchange in response to various external stimuli such as heat, endowing a new type of polymer network with combined advantages.[5] Leibler and co-workers reported silica-like malleable behavior in the associative DCNs named vitrimer—a novel material that retains constant crosslink density and good mechanical performance even at

[*] Dr. J. Luo, Dr. X. Zhao, Dr. Z. Demchuk, Dr. V. Bocharova, Prof. A. P. Sokolov
Chemical Sciences Division, Oak Ridge National Laboratory
Oak Ridge, TN-37830 (USA)

H. Ju, Dr. J. Chen, Prof. P.-F. Cao
State Key Laboratory of Organic-Inorganic Composites, Beijing University of Chemical Technology
Beijing 100029 (China)
E-mail: jiayao.chen@buct.edu.cn
caopf@buct.edu.cn

Dr. X. Chen, Prof. S. Xu
Materials Science and Engineering Program, University of California San Diego
La Jolla, CA-92093 (USA)

Dr. S. Zhao, Prof. A. P. Sokolov
Department of Chemistry, University of Tennessee
Knoxville, TN-37996 (USA)

Dr. B. Li
The Bredesen Center for Interdisciplinary Research and Graduate Education, University of Tennessee
Knoxville, TN-37996 (USA)

Dr. J.-M. Y. Carrillo, Dr. J. K. Keum
Center for Materials Sciences, Oak Ridge National Laboratory
Oak Ridge, TN-37830 (USA)

Dr. J. K. Keum
Neutron Scattering Division, Oak Ridge National Laboratory
Oak Ridge, TN-37830 (USA)

high temperatures.[6] Since then, tremendous attention has been focused on developing elastic vitrimers via different types of dynamic covalent chemistry such as transesterification,[6–7] vinylogous urethane,[8] boronic ester,[9] and disulfide exchange.[10] However, most of the reported elastic vitrimers continue to suffer from some drawbacks, such as low mechanical strength compared to the benchmark elastomers or limited recyclability, i.e., reduced physical properties after the thermal recycling. Some thermoplastic elastomers exhibit good mechanical performance and recyclability, with the trade-off of being poor solvent resistance.[11]

The classical theory of the rubber elasticity predicts for the shear modulus, G_e:

$$G_e = g\nu RT \tag{1}$$

where g and ν denote a numerical factor and moles of network strands per unit volume, respectively.[12] The latter is optimized by adjusting the functionality of elastomer precursors or by improving the network regularity to reduce the amount of dangling short chains. The dangling irregularities lower both extensibility and strength.[13] The other parameter, g includes the ratio of $\overline{r_E^2}/\overline{r_0^2}$ that is highly influenced by the length distribution of network strands; here, $\overline{r_E^2}$ is the mean square end-to-end distance of a strand, and $\overline{r_0^2}$ is a strand of the same length without being constrained by crosslinks. When strained, the network with more uniform chain length will result in more increase of $\overline{r_E^2}$, whereas for the randomly distributed chain length only short chains are mainly contributing to the stretching. For example, the slidable ring-shape crosslinks provide a dynamic adjustment of different strand lengths and achieve the improved strength and elasticity.[14] Therefore, theoretically, a defined network design with uniform crosslink distribution will afford elastomers with enhanced mechanical properties, which has been demonstrated for thermoset and gels but rarely for recyclable elastomers.[15]

Several chemical approaches were reported to overcome the bottleneck of elastic vitrimers. Since vitrimers are mainly built from dynamic covalent bonds, another feasible approach is the incorporation of non-covalent, sacrificial bonds to form a dual-dynamic elastic network.[10c,16] For example, compared with the single boronic ester-based elastic network, introduction of quadruple hydrogen bonding units 2-ureido-4[1H]-pyrimidinone (UPy) endowed significant improvement of the tensile strength (0.1 MPa to 5.5 MPa) and extensibility (175% to 235%), while such dual-dynamic elastic vitrimer still suffered limited recyclability (80% recovery after 1st cycle).[16d] In another report, a dual-dynamic elastic vitrimer with both disulfide and transesterification was fabricated with excellent recyclability (no obvious mechanical loss after 4 cycles).[10c] However, such elastic vitrimers showed relatively weak mechanical properties (tensile stress 1.7 MPa and extensibility 260%). On the other hand, Zhang and co-workers also reported an adaptable interlocking elastic vitrimer fused from two immiscible networks.[17] Compared with single-network, the interlocking elastic vitrimers demonstrated enhanced mechanical property and recyclability, i.e., tensile strength $\approx$3.5 MPa, extensibility $\approx$850%, and minor mechanical degradation upon recycling. Recently, our group also reported the ultra-recyclable, extremely tough, vitrimer-like PDMS elastomers with a high-density multiple-network structure combining both permanent chemical and dynamic physical networks.[18] With the combination of different types of dynamic covalent bonds, immiscible building blocks and network complexity, it is difficult to gain a deep physical insight, which may make such approach challenging be adapted to other polymer systems.

Herein, inspired by classical theory of rubber-like elasticity, we present a facile, universal approach to fabricate the elastic vitrimers with excellent mechanical performance and recyclability via a defined network design. The elastic vitrimers with the defined network, PDMS-disulfide-D, are built by chemically crosslinking the pre-synthesized, linear PDMS precursors with the tetra-armed PEG. By varying the PDMS chain lengths and the synthetic routes, a series of elastic vitrimers with different crosslink densities (mesh sizes) and network regularities, respectively, are obtained. The network regularity is manipulated by dangling short chains and the lengths of network strands. The optimized elastic vitrimers exhibit superior tensile stress 1.47–11.18 MPa, extensibility 290%–884%, and toughness 9.32–21.43 MJ/m^3. In addition, the PDMS-disulfide-D retain their superior mechanical performance after multiple re-processing cycles. Their extraordinary performance is due to the rational designed network architecture that has relatively uniform strand lengths between crosslinks, which is supported by comparing with the analogue possessing a random network. Moreover, considering the problem of conventional 1/e method on activation energy calculation, a unique approach is utilized here based on the segmental relaxation time, rheology shift factor, and high-frequency G'' maximum time scale. We further demonstrate that this defined-network design is universal and can be expanded to other crosslinkers. Additionally, after incorporating carbon nanotubes, the conductive elastic vitrimers show great potential as recyclable elastic materials for soft electronic devices.

Results and Discussion

PDMS is selected as the polymer backbone due to its high thermal stability and low glass transition temperature (T_g) that facilitates the analysis of network dynamics.[19] The incorporation of aromatic disulfide, here 4-aminophenyl disulfide (AFD), afford elastic networks with superior recyclability. The generated urea units during the formation of elastic network provide extra physical interaction and hence improved mechanical performance.[20] The elastic vitrimers with defined network, named PDMS$_n$-disulfide-D, involve the synthesis of linear PDMS$_n$-disulfide precursors (Scheme 1, Figures S1–S3, and Table S1). Herein, n represents different molecular weights (M_w) of PDMS-NH$_2$, e.g., M_w = 1000, 3000, and 5000 g/mol, which are considered to study the relationship between mechanical property and mesh size of defined networks, i.e., the distance between

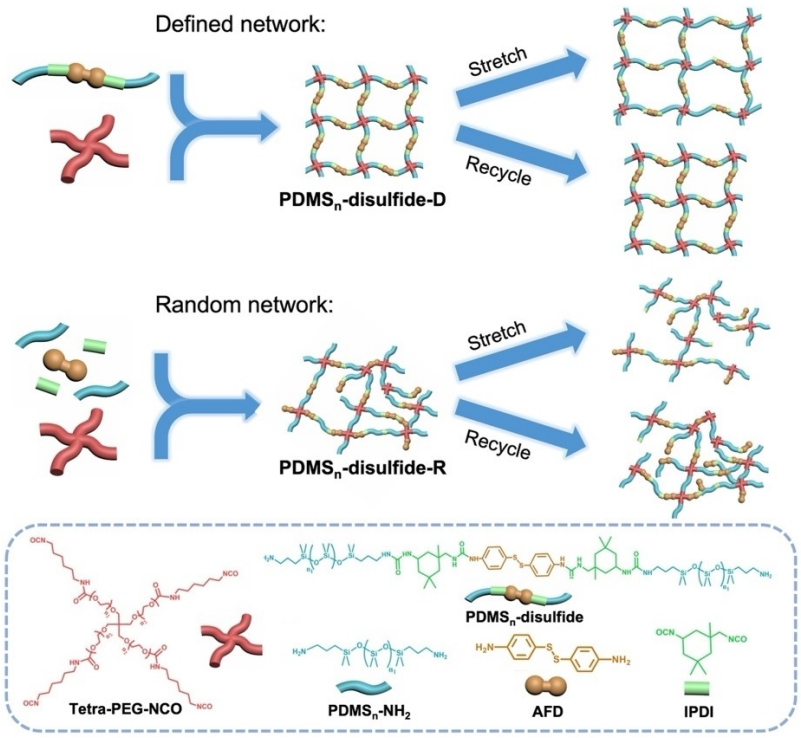

Scheme 1. Schematic illustration of the elastic vitrimers with defined network and random network.

crosslinks. As a control, elastic vitrimers with a random network, named PDMS$_n$-disulfide-R, were also synthesized from a one-pot crosslinking reaction of all four raw materials.

The obtained elastic vitrimers are highly crosslinked networks due to the nearly quantitative conversion of isocyanate-amine reaction, as evidenced by the disappearance of absorption peak of -NCO group at 2270 cm^{-1} in the FT-IR spectra (Figure 1a, Figures S4–S6). From the rheology curves (Figure 1b), the linear PDMS$_n$-disulfide precursors, e.g., PDMS$_{3000}$-disulfide, exhibit a solid-like behavior with storage modulus (G') > loss modulus (G'') at low temperature (high frequency). Upon heating to high temperature (low frequency), G'' starts to surpass G', demonstrating a typical terminal relaxation phenomenon of linear polymers,[19b,21] and the PDMS$_{3000}$-disulfide has a similar behavior (Figures S7 and S8). The elastic network of the PDMS$_{3000}$-disulfide-D shows significantly higher G' and G'' than the linear precursors (Figure 1c) and higher G' than G'' over a wide frequency range due to the solidification effect originated from chemical crosslinking (Figure S9). No obvious thermal degradation below 270 °C is observed for the designed elastic vitrimers (Figure S10), and the PDMS-disulfide-D networks derived from longer PDMS chains exhibit higher thermal stability because of high PDMS content, consistent with our previous works,[19b] as well as excellent solvent resistance (Figure S11).

The SAXS curve of PDMS$_{3000}$-disulfide-D shows a relatively broad peak (Figure 1d), and the peak position ($q_{max}=0.044$ Å^{-1}) was fit using Broad Peak Model[22] to calculate the characteristic correlation distance ($d=2\pi/q_{max}$) as 14.6 nm. The mesh size of PDMS$_{3000}$-disulfide-D network is estimated as 11.7 nm and 37.6 nm based on the Gaussian coil and extended chain models, respectively. Among the multiple segments in the defined network, PDMS and PEG are the dominant segments with distinct electron densities. Therefore, the SAXS peak which reflects spatial correlations between the segments could be attributed to the periodic alternation of PDMS and PEG blocks, and this micro-phase separation is invisible in the atomic force microscopy (AFM) image at such length scale (Figure 1e). To support this assumption, another defined network synthesized solely from PDMS-NH$_2$ ($M_w=5000$ g/mol) and tetra-PEG-NCO was also prepared (PDMS-PEG in Figure S12). The SAXS curve of the PDMS-PEG shows a similar peak position as that of the PDMS$_{3000}$-disulfide-D. Hence, the defined network with structured meshes and high crosslink density prevents the formation of large phase separation in the system. On the other hand, the PDMS$_{3000}$-disulfide-R exhibits an intense peak at $q=0.020$ Å^{-1}, i.e., $d=31.4$ nm (Figure 1d). Its AFM image also shows severe aggregation morphology (Figure 1f), therefore, the SAXS peak in PDMS-disulfide-R is likely ascribed to the significant phase separation with larger average center-to-center distance during network formation. The SAXS data were fit using a combined lognormal sphere model with structure factor to account for phase separated domains[23] and Broad Peak Model for network structure. The model fit indicated the existence of spherical domains with the mean diameter of 28 nm (Figure S13), and the correlation distance between the centers of the clusters is 32 nm. In addition, the SAXS curves of PDMS$_{1000}$-disulfide-R and PDMS$_{5000}$-disulfide-R

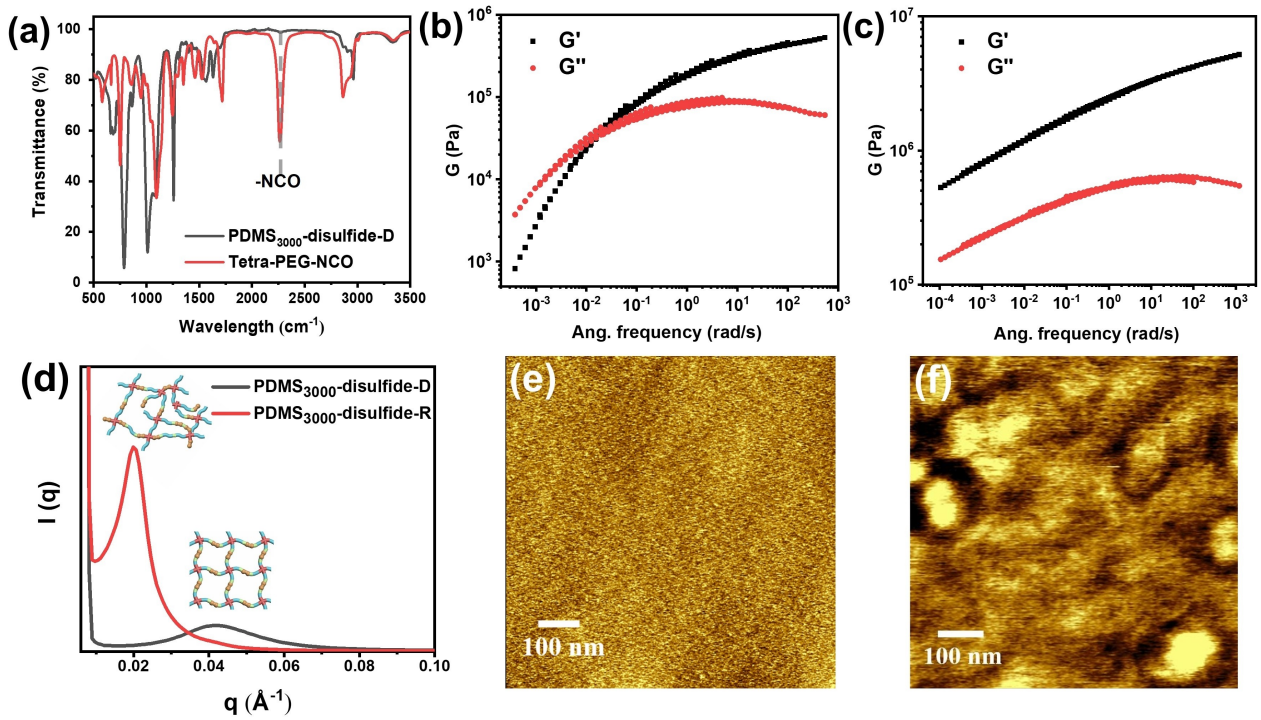

Figure 1. (a) FT-IR spectra of the tetra-PEG-NCO and $PDMS_{3000}$-disulfide-D. The dashed line at 2270 cm^{-1} represents the signal from isocyanates. (b) Frequency sweep of linear $PDMS_{3000}$-disulfide precursor. (c) Frequency sweep of $PDMS_{3000}$-disulfide-D. The reference temperature is 30 °C. (d) SAXS curves obtained from $PDMS_{3000}$-disulfide-D and $PDMS_{3000}$-disulfide-R. AFM images of (e) the $PDMS_{3000}$-disulfide-D and (f) the $PDMS_{3000}$-disulfide-R.

also reveal the significant phase separation ascribed to the comparatively gentle slope and q_{max} peak, respectively (Figure S14). The distinctive morphologies between the defined and random networks have a significant impact on their mechanical performance and recyclability.

The elastic vitrimers with the defined-network architecture show excellent mechanical performance as illustrated in Figure 2a and Table 1. For example, the $PDMS_{1000}$-disulfide-D demonstrates a tensile stress of 11.18 ± 0.57 MPa and extensibility of 290 ± 4 %. With longer PDMS chains, the extensibility further increases to 532 ± 1 % and 884 ± 18 %, while the tensile stress decreases to 6.68 ± 0.34 MPa and 1.47 ± 0.06 MPa for $PDMS_{3000}$-disulfide-D and $PDMS_{5000}$-disulfide-D, respectively. Meanwhile, their overall toughness decreases from 21.43 ± 0.33 MJ/m^3 to 19.45 ± 0.71 MJ/m^3 and 9.32 ± 0.22 MJ/m^3 when switching the PDMS blocks from 1000 to 3000 and 5000 g/mol, respectively. Although longer PDMS chains, i.e., larger mesh size, can enhance the stretchability, the reduced crosslink density renders reduced tensile stress and toughness, which follows the common trend of traditional thermoset elastomers.[24] The designed elastic vitrimers show decent elastic recovery with leftover strain < 15 % after 10 cycles of 100 % elongation processes (Figure 2b). Comparing with the cases using $PDMS_{1000}$ and $PDMS_{5000}$ (Figures S15 and S16), the elastic vitrimers with shorter strand lengths between crosslinks exhibit reduced hysteresis loss, suggesting the lower dissipation energy and better elastic recovery. All three vitrimer samples with different chains lengths show distinct hysteresis loops in the first cyclic tests, followed by gradually reduced hysteresis loss in the afterward cyclic test. The hysteresis loops can be explained by the energy dissipation caused by disassociation of dynamic bonds, which cannot be reformed during the short time scale. Moreover, full recovery of original length can be achieved after relaxing the stretched film for 3 min (Figure 2c). Benefited from the rational network design, the $PDMS_n$-disulfide-D achieve significantly higher mechanical toughness and improved recyclability than the previously reported PDMS-based vitrimers (Figure 2d and Table S2).[25] The PDMS-disulfide-D even show superior mechanical

Table 1: Mechanical properties of designed elastic vitrimers.

Sample	Young's Modulus [MPa]	Elongation at Break [%]	Toughness [MJ/m^3]	Ultimate Tensile Strength [MPa]
$PDMS_{1000}$-disulfide-D	26.74 ± 1.30	290 ± 4	21.43 ± 0.33	11.18 ± 0.57
$PDMS_{3000}$-disulfide-D	6.28 ± 0.35	532 ± 17	19.45 ± 0.71	6.68 ± 0.34
$PDMS_{5000}$-disulfide-D	1.45 ± 0.09	884 ± 18	9.32 ± 0.22	1.47 ± 0.06
$PDMS_{3000}$-disulfide-R	3.33 ± 0.37	150 ± 12	1.53 ± 0.22	1.63 ± 0.24

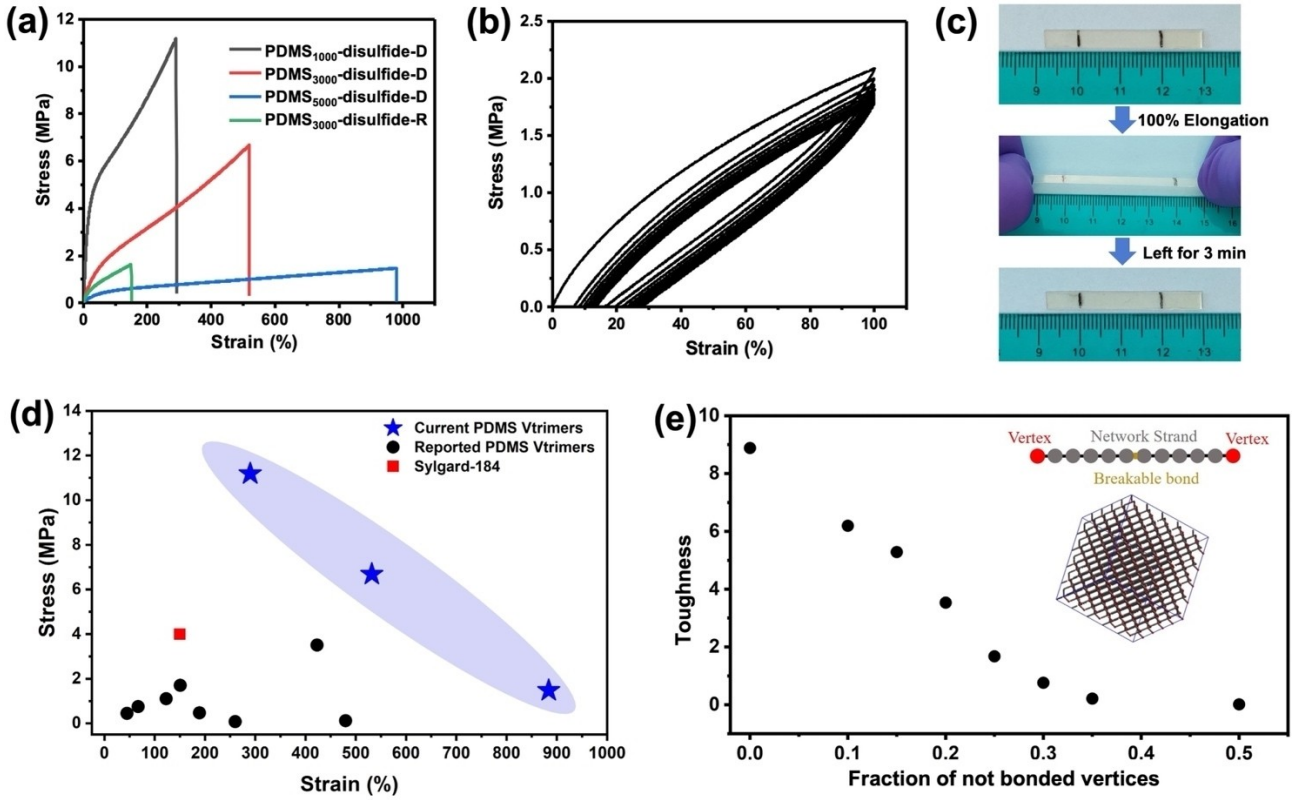

Figure 2. (a) Strain-stress curves of the elastic vitrimers with defined and random networks. (b) Hysteresis test of the $PDMS_{3000}$-disulfide-D. (c) Photos showing the stretching and relaxation process of the elastic vitrimers. (d) Comparison of mechanical performance between reported PDMS vitrimers and current elastic vitrimers. (e) Schematic illustration of the diamond network, and the relationship between toughness and crosslink density (fraction of not bonded vertices) in the elastic network. The yellow breakable bond in the middle represents the exchangeable disulfide bond.

performance than the commercial silicone-based thermosets.[26] For example, the $PDMS_{1000}$-disulfide-D and the $PDMS_{3000}$-disulfide-D exhibit higher mechanical performance than widely used silicone Sylgard-184 (tensile stress 6.5 MPa vs. 4.0 MPa, extensibility 500 % vs. ≈150 %). Although the silicone elastomer Elastosil-M4630 (≈4.5 MPa and ≈780 %) exhibits comparable tensile stress to the $PDMS_{3000}$-disulfide-D, the low optical transparency and non-recyclability limit its utilization.

One major contributor to improved mechanical properties of the PDMS-disulfide-D is their defined network architecture with relatively uniform strand lengths between crosslinks. With the same chemical component and PDMS chain length, the $PDMS_{3000}$-disulfide-D shows significantly improved tensile stress (6.68 ± 0.34 MPa vs. 1.63 ± 0.24 MPa) and extensibility (532 ± 17 % vs. 150 ± 12 %) with overall toughness 12.7 times higher than the control group, i.e., $PDMS_{3000}$-disulfide-R. As illustrated in the SAXS and AFM results (Figure 1d–1f), the random network shows significant phase separation, indicating aggregation of crosslinkers, that is to say, higher crosslink densities occur in some locations. During uniaxial deformation, the sites with different crosslink densities show different responses to external forces, and "weak" location will fail first. To support the assumption, coarse-grained molecular dynamics (MD) simulation on a diamond network is performed to provide a microscopic understanding between network parameters and mechanical performance (details in Supporting Information, Figures S17–S19).[27] As shown in Figure 2e, the overall toughness of network decreases rapidly with the increased number of unbonded chains (dangling chains in vertices), i.e., lower crosslink density. The results suggest that the elastic vitrimers with random network only tolerate a limited force due to the local defects. In contrast, the elastic vitrimers with defined network exhibit a relatively homogeneous distribution of crosslinks, contributing to excellent mechanical performance.

The temperature response of network dynamics is first evaluated by dynamic mechanical analysis (DMA), and Figure 3a shows the network illustrations of the samples. The storage modulus (E') of the elastic vitrimers typically exhibits constant rubbery plateaus over a wide range of temperatures above T_g,[5c,28] while the $PDMS_{3000}$-disulfide-D exhibits a gradual decrease of E' above T_g (Figure 3b). This might be explained by the significantly enhanced network dynamics from the synergic effect of two types of dynamic bonds, i.e., disulfide exchange and hydrogen bonding, consistent with previous report.[10c] The tan (δ) of $PDMS_{3000}$-disulfide-D exhibits two transition peaks, and the one at −120 °C is attributed to the glass transition of the PDMS

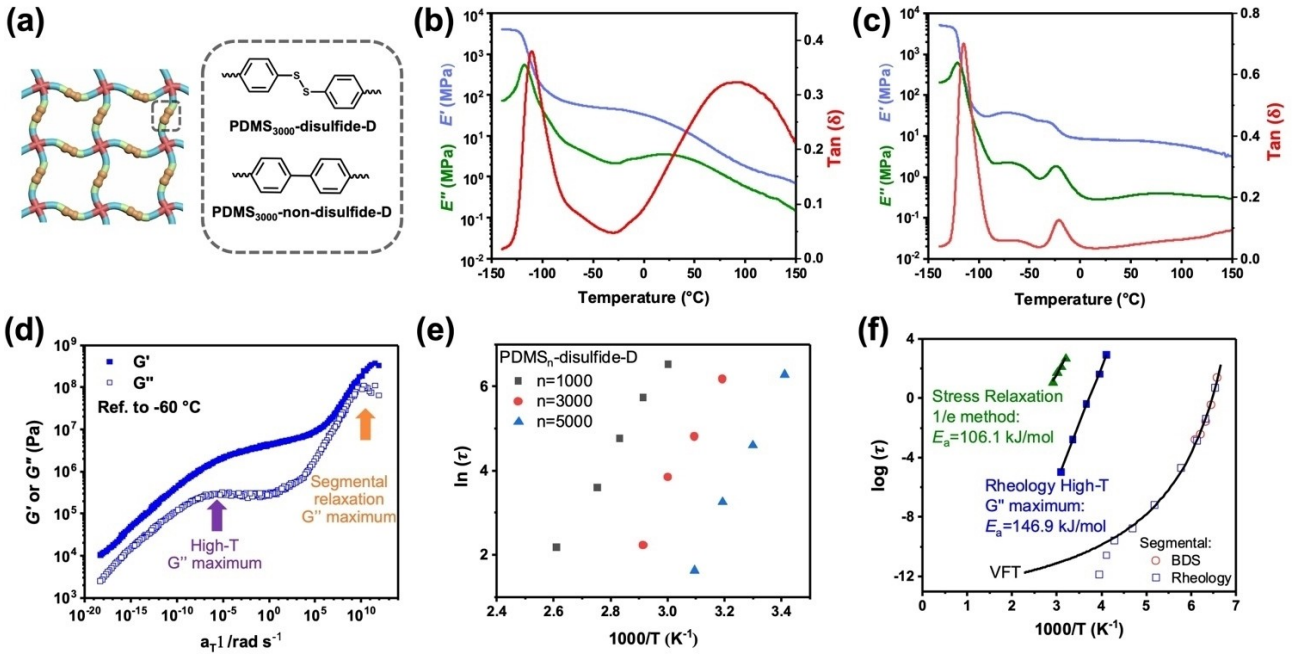

Figure 3. (a) Schematic illustration of disulfide-contain network and control sample. (b) DMA results of $PDMS_{3000}$-disulfide-D. (c) DMA results of $PDMS_{3000}$-non-disulfide-D, the small tan (δ) peak at around −30 °C is likely related to PEG chain. (d) Master curves of $PDMS_{3000}$-disulfide-D. (e) Arrhenius plot of ln (τ) *vs.* 1000/T. (f) Combined plots of the relationship between log (τ) and 1000/T from different methods in $PDMS_{3000}$-disulfide-D.

chains. The second broad peak at 80 °C should not be associated with the melting process of PEG segments due to the absence of a transition peak from 0 °C to 150 °C in the DSC curves (Figures S20–S22). To unravel the origin of such broad peak, an elastic network was prepared by switching disulfide-containing ADF to non-disulfide benzidine, i.e., $PDMS_{3000}$-non-disulfide-D, and no peak at 80 °C is observed in its DMA curve (Figure 3c), suggesting that the broad peak is related to the dynamic exchange of disulfides. Such dynamic bond exchange leads to a non-terminal relaxation process after the rubbery behavior as indicated by the rheology result. Similar DMA responses are observed from $PDMS_n$-disulfide-D with different M_w of PDMS chains (Figures S23 and S24).

The dynamic processes of elastic vitrimers are further investigated by the master curves of rheology data, and the typical curve of $PDMS_{3000}$-disulfide-D is shown in Figure 3d. At the high-frequency range, the maximum peak of G'' is attributed to the segmental relaxation, and the corresponding frequency sweep is at −120 °C. As frequency decreases (or temperature increases), the glass-to-rubber transition, rubbery plateau, and another G'' maximum are consecutively observed, consistent with DMA result. The glass-to-rubber transition was due to the devitrification of PDMS segments that led to the elastic rubbery state. Especially, this low-frequency G'' maximum within the measurement window does not correspond to the terminal flow as the following G' is still parallel to and higher than G''. Importantly, the rheology result of the control network with non-disulfide benzidine does not show such a G'' maximum but only a wide rubbery plateau, indicating that this process is related to the disulfide bond exchange.[29] Therefore, the bond exchange does not necessarily lead to a terminal relaxation and flow behavior where bond exchanges predominate. Many previous studies with dynamic bonds use 'viscosity' estimated from stress relaxation while this approach is inappropriate if the system does not show terminal relaxation (e.g., Figure 3e). It is also interesting to point out that the frequency dependence of G' and G'' are parallel to each other in the double logarithmic plot presenting gel-like behavior, and their slopes are 0.2, in agreement with predictions of Winter's gel point theory.[30] Thus, it will be of great interest to explore the nature of this gelation process. In addition, the apparent moles of strands between crosslinks, proportionally relating to the crosslink densities, of the elastic vitrimers can be calculated by substituting G' in Equation (1) with the value at rubbery plateau extracted from the master curves. The apparent moles of strands are 2.54×10^{-3} and 1.35×10^{-3} mol/cm^3 for the $PDMS_{3000}$-disulfide-D and $PDMS_{3000}$-disulfide-R (Figure S25), respectively.

The topological rearrangement at elevated temperatures reflects the temperature dependence of disulfide exchange and can be quantified by the apparent activation energy (E_a).[5b,c,e] The E_a can be calculated using the Arrhenius equation: $\tau_b = Ae^{E_a/RT}$, where τ_b is the characteristic time of bond exchange, A is a prefactor, R is the gas constant, and T is the temperature. The traditional 1/e method using stress relaxation experiments was firstly applied to determine τ as the time when the normalized stress decreases to 37 % (1/e) of the initial value. The ln (τ) shows a good linear relationship versus the 1000/T (Figure 3e, Figures S26–S28), and

their slopes give the apparent activation energies of 94.8 kJ/mol, 106.1 kJ/mol, and 120.5 kJ/mol for the $PDMS_{1000}$-disulfide-D, $PDMS_{3000}$-disulfide-D, and $PDMS_{5000}$-disulfide-D, respectively (Figure S29). The calculated values are within the ranges in various reported disulfide-containing vitrimers (50–200 kJ/mol).[5c]

However, there is a main problem with the 1/*e* method that the initial modulus utilized to normalize the corresponding relaxation process may not be captured by the stress relaxation measurement window. Evidence is shown by comparing against the rheology relaxation time in Figure 3f, and the 1/*e* method gives higher relaxation time and lower apparent activation energy. The rheology relaxation time is more reliable because the high-frequency G'' maximum that corresponds to the bond exchange is directly observed in the measurement window. The temperature dependence of relaxation time was represented by the time-temperature-superposition shift factor (details in Supporting Information, Figure S30). Notably, Figure 3f revealed that the relaxation time for bond exchange was accessible by the experimental window, which presumably provides additional contribution to the increased extensibility and toughness as the network rearranges to adapt to the tensile stress. Moreover, it is worth pointing out that the apparent activation energy here accounts not only the bond exchange process but also the segmental dynamics of backbones, whose characteristic time, τ_a, is the segmental relaxation time estimated from the rheology shift factor and high-frequency G″ maximum time scale that agreed well with the segmental relaxation probed by broadband dielectric spectroscopy (BDS, Figure S31). Taking this into consideration, we modified the traditional Arrhenius equation with the pre-factor as the segmental relaxation time, τ_a. It is interpreted that the temperature-dependent segmental dynamics allow efficient exchange of disulfide bonds with obtained $\tau_b = \tau_a e^{E_a/RT}$.[31] With τ_a (extrapolated by Vogel-Fulcher-Tammann equation) and τ_b, the activation energy of disulfide exchange in $PDMS_{3000}$-disulfide-D is recalculated to be 122.0 kJ/mol (details in Supporting Information).

Elastic vitrimers can be thermally reprocessed due to the bond exchange, leading to the sustainable feature of polymeric materials.[4f,5d,32] In a typical procedure (Figure 4a), the film of elastic vitrimers with the defined network (e.g., $PDMS_{3000}$-disulfide-D) is broken into small pieces. Upon application of pressure and temperature, the film shows a fully recovered mechanical performance, demonstrating excellent re-processability (Figure 4b). Such a re-processing process can repeat five cycles with no obvious mechanical loss. All elastic vitrimers with the defined networks show excellent re-processability regardless of PDMS lengths (Figures S32 and S33). Comparatively, the elastic vitrimer with random network, i.e., $PDMS_{3000}$-disulfide-R, exhibits a continuous decrease of mechanical performance with increased reprocessing cycles (Figure 4c).

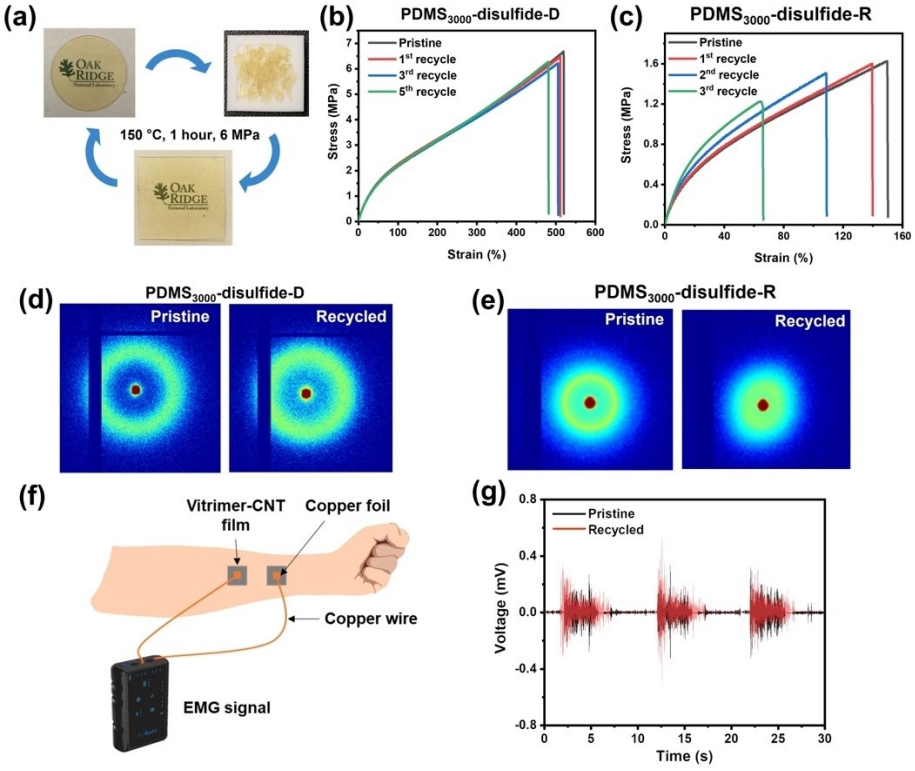

Figure 4. (a) Photos showing a typical reprocessing procedure. (b) Strain-stress curves of $PDMS_{3000}$-disulfide-D after different reprocessing cycles. (c) Strain-stress curves of $PDMS_{3000}$-disulfide-R after various reprocessing cycles. (d) 2D SAXS patterns of $PDMS_{3000}$-disulfide-D before and after recycling (e) 2D SAXS patterns of $PDMS_{3000}$-disulfide-R before and after recycling (f) Schematic illustration of EMG sensor setup. (g) Comparison of the EMG signal between pristine and recycled $PDMS_{3000}$-disulfide-D.

The distinct results herein suggest better re-processability of the vitrimers with defined-network design. As illustrated in 2D SAXS images (Figure 4d and 4e), the $PDMS_{3000}$-disulfide-D exhibits almost complete morphology recovery and isotropic orientation after thermal reprocessing, indicating that the defined network design retains network regularity after initial thermal cycles. The slightly reduced mechanical toughness of $PDMS_{3000}$-disulfide-D, especially after 5 cycles, may still manifest the decreased structure regularity with increasing reprocessing cycles. On the contrary, the recycled $PDMS_{3000}$-disulfide-R exhibits anisotropic orientation and different morphology other than its original state, consistent with the mechanical results from processability tests. The anisotropic orientation is possibly due to the re-organization of large clusters in network. To demonstrate the universality of the defined network design, the elastic vitrimers with disulfide containing PDMS chains and different types of crosslinkers (e.g., terminated with epoxy and acrylate) were also synthesized. As expected, the elastic vitrimers with the same network design while different chemical components also exhibit excellent re-processability (Figures S34 and S35), suggesting the applicability of the proposed network design to other polymer systems.

By incorporating carbon nanotubes (CNT) into $PDMS_{3000}$-disulfide-D, the resultant elastomers show good electronic conductivity across a wide frequency range (Figures S36 and S37), providing a potential opportunity for fabricating various soft electronics.[33] Herein, an electromyography (EMG) sensor was fabricated from vitrimer-CNT composites (Figure 4f), and the electrochemical signals are obtained with voltage *vs.* time curve. The EMG sensor can capture the periodic activity of muscles with a relatively high signal-to-noise ratio. After thermal reprocessing, the recycled composites exhibit comparable performance as the pristine ones.[34] Such demonstration indicates the great potential of designed vitrimers as sustainable elastic materials for different applications.

Conclusion

A series of elastic vitrimers with defined-network architecture are designed from tetra-armed crosslinkers and pre-synthesized PDMS-based linear precursors, with disulfide as dynamic chemical bonds and urethane and urea units as physical bonding. The PDMS-disulfide-D prepared from different lengths of PDMS precursors show excellent mechanical performance, i.e., tensile stress 1.47–11.18 MPa, extensibility 290 %–884 %, and toughness 9.32–21.43 MJ/m^3, superior to previously reported PDMS-based vitrimers and commercially available silicone elastomers. The defined network vitrimers also exhibit excellent re-processability with no obvious loss of mechanical properties after 5 reprocessing cycles. The extraordinary performance of PDMS-disulfide-D comes from their rational designed architecture with uniform crosslink distribution as confirmed by comparing to control samples with random-network configuration and coarse-grained MD simulation. A dynamic bond exchange process which leads to a non-terminal relaxation and gel-like behavior is observed from the rheology and DMA curves. Instead of the conventional $1/e$ method that has some limitations, the activation energy of disulfide exchange is estimated from the rheology relaxation time obtained from the high-temperature G'' maximum along with the segmental relaxation time obtained from the rheology shift factor and high-frequency G'' maximum time scale. Additionally, we further show that this rational defined-network design can be utilized to build elastic networks with other tetra-armed crosslinkers such as epoxy- and acrylate-based ones. Enabling electronic conducting by incorporating carbon nanotubes, the design elastic vitrimers also demonstrate its great potential as recyclable soft electronics.

Inspired by classical theory of elasticity, the strategy of designing elastic vitrimers with defined network will provide a guidance for developing soft materials with enhanced mechanical performance and improved recyclability towards applications that includes but not limited to sensors, electronics, and smart materials. Such demonstration significantly correlates the physical theory, structure design, polymer property, and functional materials. Moreover, although widely adopted in numerous publications, the $1/e$ method on activation energy analysis is not accurate as revealed in the study. The unique physical calculation on dynamic process of such polymer network here will also pave a fresh insight for accurate analysis for vitrimers and other dynamic/adaptable materials.

Supporting Information

Synthetic scheme, NMR, GPC, FT-IR, TGA, DSC, rheology, DMA, recyclability, and simulation results can be found in Supporting Information.

Acknowledgements

J. Luo, X. Zhao, and H. Ju contributed equally to the work. This research was supported by the National Natural Science Foundation of China (grant no. 52373275 and 52303290). This research at the Oak Ridge National Laboratory managed by UT Battelle for the U.S. Department of Energy (DOE) under Contract No. DE-AC05-00OR22725, was sponsored by the Laboratory Directed Research and Development Program at Oak Ridge National Laboratory. The research was also supported by Fundamental Research Funds for the Central Universities (buctrc202222 and buctrc202310). A.P.S. acknowledge financial support for data analysis and interpretation by NSF Polymer program (award DMR-1904657). This research used the resources of the Center for Nanophase Materials Sciences (CNMS) and Spallation Neutron Source (SNS), which are DOE Office of Science User Facilities. The material was partially based on research sponsored by Air Force Research Laboratory under agreement number FA8650-18-2-5402. The authors thank Dr. Chenyang Liu and Dr. Baoqing Zhang from University of Chinese

Academy of Science, China for the rheology characterization.

Conflict of Interest

The authors declare no conflict of interest.

Keywords: Defined Network · Polydimethylsiloxane · Recyclable Polymer · Tough Elastomer · Vitrimers

[1] a) Z. Zhang, N. Ghezawi, B. Li, S. Ge, S. Zhao, T. Saito, D. Hun, P.-F. Cao, *Adv. Funct. Mater.* **2021**, *31*, 2006298; b) W.-G. Chen, H.-J. Wei, J. Luo, Y. Chen, P.-F. Cao, *Macromolecules* **2021**, *54*, 3169; c) K. Yu, A. Xin, H. Du, Y. Li, Q. Wang, *NPG Asia Mater.* **2019**, *11*, 7; d) H. Frey, T. Johann, *Polym. Chem.* **2020**, *11*, 8.

[2] a) Y. Wang, G. A. Ameer, B. J. Sheppard, R. Langer, *Nat. Biotechnol.* **2002**, *20*, 602; b) J. Kang, D. Son, G.-J. N. Wang, Y. Liu, J. Lopez, Y. Kim, J. Y. Oh, T. Katsumata, J. Mun, Y. Lee, L. Jin, J. B. H. Tok, Z. Bao, *Adv. Mater.* **2018**, *30*, 1706846; c) Q. Ma, S. Liao, Y. Ma, Y. Chu, Y. Wang, *Adv. Mater.* **2021**, *33*, 2102096; d) J.-F. Yin, H. Xiao, P. Xu, J. Yang, Z. Fan, Y. Ke, X. Ouyang, G. X. Liu, T. L. Sun, L. Tang, S. Z. D. Cheng, P. Yin, *Angew. Chem. Int. Ed.* **2021**, *60*, 22212; e) Z. Lin, H. Deng, Y. Hou, X. Liu, R. Xu, H. Xiang, Z. Peng, M. Rong, M. Zhang, *J. Mater. Chem. A* **2022**, *10*, 11019.

[3] a) G. Holden, in *Rubber technology*, Springer, Berlin, **1987**, pp. 465; b) Q. Chen, L. Zhu, H. Chen, H. Yan, L. Huang, J. Yang, J. Zheng, *Adv. Funct. Mater.* **2015**, *25*, 1598; c) J. Zhu, S. Zhao, J. Luo, W. Niu, J. T. Damron, Z. Zhang, M. A. Rahman, M. A. Arnould, T. Saito, R. Advincula, A. P. Sokolov, B. G. Sumpter, P.-F. Cao, *CCS Chem.* **2023**, *5*, 1841.

[4] a) Y. Jin, C. Yu, R. J. Denman, W. Zhang, *Chem. Soc. Rev.* **2013**, *42*, 6634; b) C. J. Kloxin, T. F. Scott, B. J. Adzima, C. N. Bowman, *Macromolecules* **2010**, *43*, 2643; c) C. J. Kloxin, C. N. Bowman, *Chem. Soc. Rev.* **2013**, *42*, 7161; d) S. J. Rowan, S. J. Cantrill, G. R. L. Cousins, J. K. M. Sanders, J. F. Stoddart, *Angew. Chem. Int. Ed.* **2002**, *41*, 898; e) N. Zheng, Y. Xu, Q. Zhao, T. Xie, *Chem. Rev.* **2021**, *121*, 1716; f) P. Chakma, D. Konkolewicz, *Angew. Chem. Int. Ed.* **2019**, *58*, 9682.

[5] a) M. Podgórski, B. D. Fairbanks, B. E. Kirkpatrick, M. McBride, A. Martinez, A. Dobson, N. J. Bongiardina, C. N. Bowman, *Adv. Mater.* **2020**, *32*, 1906876; b) M. Guerre, C. Taplan, J. M. Winne, F. E. Du Prez, *Chem. Sci.* **2020**, *11*, 4855; c) G. M. Scheutz, J. J. Lessard, M. B. Sims, B. S. Sumerlin, *J. Am. Chem. Soc.* **2019**, *141*, 16181; d) Y. Jin, Z. Lei, P. Taynton, S. Huang, W. Zhang, *Matter* **2019**, *1*, 1456; e) W. Denissen, J. M. Winne, F. E. Du Prez, *Chem. Sci.* **2016**, *7*, 30.

[6] D. Montarnal, M. Capelot, F. Tournilhac, L. Leibler, *Science* **2011**, *334*, 965.

[7] a) J. L. Self, C. S. Sample, A. E. Levi, K. Li, R. Xie, J. R. de Alaniz, C. M. Bates, *J. Am. Chem. Soc.* **2020**, *142*, 7567; b) L. Cao, J. Fan, J. Huang, Y. Chen, *J. Mater. Chem. A* **2019**, *7*, 4922; c) C. A. Tretbar, J. A. Neal, Z. Guan, *J. Am. Chem. Soc.* **2019**, *141*, 16595.

[8] a) W. Denissen, G. Rivero, R. Nicolaÿ, L. Leibler, J. M. Winne, F. E. Du Prez, *Adv. Funct. Mater.* **2015**, *25*, 2451; b) W. Denissen, M. Droesbeke, R. Nicolaÿ, L. Leibler, J. M. Winne, F. E. Du Prez, *Nat. Commun.* **2017**, *8*, 14857; c) W. Denissen, I. De Baere, W. Van Paepegem, L. Leibler, J. Winne, F. E. Du Prez, *Macromolecules* **2018**, *51*, 2054.

[9] a) J. J. Cash, T. Kubo, A. P. Bapat, B. S. Sumerlin, *Macromolecules* **2015**, *48*, 2098; b) M. Röttger, T. Domenech, R. van der Weegen, A. Breuillac, R. Nicolaÿ, L. Leibler, *Science* **2017**, *356*, 62; c) O. R. Cromwell, J. Chung, Z. Guan, *J. Am. Chem. Soc.* **2015**, *137*, 6492; d) J. V. Accardo, E. R. McClure, M. A. Mosquera, J. A. Kalow, *J. Am. Chem. Soc.* **2020**, *142*, 19969; e) S. Wu, H. Yang, W.-S. Xu, Q. Chen, *Macromolecules* **2021**, *54*, 6799.

[10] a) Z. Q. Lei, H. P. Xiang, Y. J. Yuan, M. Z. Rong, M. Q. Zhang, *Chem. Mater.* **2014**, *26*, 2038; b) Z. Wang, H. Tian, Q. He, S. Cai, *ACS Appl. Mater. Interfaces* **2017**, *9*, 33119; c) M. Chen, L. Zhou, Y. Wu, X. Zhao, Y. Zhang, *ACS Macro Lett.* **2019**, *8*, 255; d) B. T. Michal, C. A. Jaye, E. J. Spencer, S. J. Rowan, *ACS Macro Lett.* **2013**, *2*, 694.

[11] a) Z. Li, Y.-L. Zhu, W. Niu, X. Yang, Z. Jiang, Z.-Y. Lu, X. Liu, J. Sun, *Adv. Mater.* **2021**, *33*, 2101498; b) X. Wang, S. Zhan, Z. Lu, J. Li, X. Yang, Y. Qiao, Y. Men, J. Sun, *Adv. Mater.* **2020**, *32*, 2005759.

[12] J. D. Ferry, *Viscoelastic properties of polymers*, John Wiley & Sons, New York, **1980**.

[13] A. L. Andrady, M. A. Llorente, M. A. Sharaf, R. R. Rahalkar, J. E. Mark, J. L. Sullivan, C. U. Yu, J. R. Falender, *J. Appl. Polym. Sci.* **1981**, *26*, 1829.

[14] a) Y. Okumura, K. Ito, *Adv. Mater.* **2001**, *13*, 485; b) P. Hu, J. Madsen, Q. Huang, A. L. Skov, *ACS Macro Lett.* **2020**, *9*, 1458; c) J. Zhao, Z. Zhang, L. Cheng, R. Bai, D. Zhao, Y. Wang, W. Yu, X. Yan, *J. Am. Chem. Soc.* **2022**, *144*, 872.

[15] G. A. Parada, X. Zhao, *Soft Matter* **2018**, *14*, 5186.

[16] a) J.-H. Chen, X.-P. An, Y.-D. Li, M. Wang, J.-B. Zeng, *Chin. J. Polym. Sci.* **2018**, *36*, 641; b) A. Breuillac, A. Kassalias, R. Nicolaÿ, *Macromolecules* **2019**, *52*, 7102; c) Y. Chen, Z. Tang, Y. Liu, S. Wu, B. Guo, *Macromolecules* **2019**, *52*, 3805; d) C. Zhang, Z. Yang, N. T. Duong, X. Li, Y. Nishiyama, Q. Wu, R. Zhang, P. Sun, *Macromolecules* **2019**, *52*, 5014; e) K. Cao, G. Liu, *Macromolecules* **2017**, *50*, 2016; f) P. Song, H. Wang, *Adv. Mater.* **2020**, *32*, 1901244; g) K. Liu, L. Cheng, N. Zhang, H. Pan, X. Fan, G. Li, Z. Zhang, D. Zhao, J. Zhao, X. Yang, Y. Wang, R. Bai, Y. Liu, Z. Liu, S. Wang, X. Gong, Z. Bao, G. Gu, W. Yu, X. Yan, *J. Am. Chem. Soc.* **2021**, *143*, 1162; h) J. Luo, Z. Demchuk, X. Zhao, T. Saito, M. Tian, A. P. Sokolov, P.-F. Cao, *Matter* **2022**, *5*, 1391.

[17] W. L. Peng, Y. You, P. Xie, M. Z. Rong, M. Q. Zhang, *Macromolecules* **2020**, *53*, 584.

[18] Q. Chen, X. Zhao, B. Li, A. P. Sokolov, M. Tian, R. Advincula, P.-F. Cao, *Matter* **2023**, *6*, 1.

[19] a) C.-H. Li, C. Wang, C. Keplinger, J.-L. Zuo, L. Jin, Y. Sun, P. Zheng, Y. Cao, F. Lissel, C. Linder, X.-Z. You, Z. Bao, *Nat. Chem.* **2016**, *8*, 618; b) P.-F. Cao, B. Li, T. Hong, J. Townsend, Z. Qiang, K. Xing, K. D. Vogiatzis, Y. Wang, J. W. Mays, A. P. Sokolov, T. Saito, *Adv. Funct. Mater.* **2018**, *28*, 1800741.

[20] a) Y. Zhuo, Z. Xia, Y. Qi, T. Sumigawa, J. Wu, P. Šesták, Y. Lu, V. Håkonsen, T. Li, F. Wang, W. Chen, S. Xiao, R. Long, T. Kitamura, L. Li, J. He, Z. Zhang, *Adv. Mater.* **2021**, *33*, 2008523; b) C. Kim, S. Nakagawa, M. Seshimo, H. Ejima, H. Houjou, N. Yoshie, *Macromolecules* **2020**, *53*, 4121; c) J. Wu, L.-H. Cai, D. A. Weitz, *Adv. Mater.* **2017**, *29*, 1702616; d) Y. Chen, Z. Guan, *Chem. Commun.* **2014**, *50*, 10868.

[21] Z. Zhang, J. Luo, S. Zhao, S. Ge, J.-M. Y. Carrillo, J. K. Keum, C. Do, S. Cheng, Y. Wang, A. P. Sokolov, P.-F. Cao, *Matter* **2022**, *5*, 237.

[22] F. Horkay, B. Hammouda, *Colloid Polym. Sci.* **2008**, *286*, 611.

[23] D. L. Price, *Methods of experimental physics*, Academic Press, San Diego, **1987**.

[24] G. J. Lake, A. G. Thomas, D. Tabor, *Proc. R. Soc. London Ser. A* **1967**, *300*, 108.

[25] a) B. Krishnakumar, M. Singh, V. Parthasarthy, C. Park, N. G. Sahoo, G. J. Yun, S. Rana, *Nanoscale Adv.* **2020**, *2*, 2726; b) Y. Spiesschaert, M. Guerre, L. Imbernon, J. M. Winne, F. Du Prez, *Polymer* **2019**, *172*, 239; c) Z. Feng, B. Yu, J. Hu, H.

Zuo, J. Li, H. Sun, N. Ning, M. Tian, L. Zhang, *Ind. Eng. Chem. Res.* **2019**, *58*, 1212; d) T. Stukenbroeker, W. Wang, J. M. Winne, F. E. Du Prez, R. Nicolaÿ, L. Leibler, *Polym. Chem.* **2017**, *8*, 6590; e) H. Zhang, C. Cai, W. Liu, D. Li, J. Zhang, N. Zhao, J. Xu, *Sci. Rep.* **2017**, *7*, 11833; f) T. Patel, M. P. Kim, J. Park, T. H. Lee, P. Nellepalli, S. M. Noh, H. W. Jung, H. Ko, J. K. Oh, *ACS Nano* **2020**, *14*, 11442; g) J. Sun, X. Pu, M. Liu, A. Yu, C. Du, J. Zhai, W. Hu, Z. L. Wang, *ACS Nano* **2018**, *12*, 6147; h) Z. Wang, Y. Liu, D. Zhang, K. Zhang, C. Gao, Y. Wu, *Compos. Sci. Technol.* **2021**, *216*; i) D. Zhang, F. Vashahi, E. Dashtimoghadam, X. Hu, C. J. Wang, J. Garcia, A. V. Bystrova, M. Vatankhah-Varnoosfaderani, F. A. Leibfarth, S. S. Sheiko, *Angew. Chem. Int. Ed.* **2023**, *62*, e202217941.

[26] S. Park, K. Mondal, R. M. Treadway, V. Kumar, S. Ma, J. D. Holbery, M. D. Dickey, *ACS Appl. Mater. Interfaces* **2018**, *10*, 11261.

[27] a) S. Plimpton, *J. Comput. Phys.* **1995**, *117*, 1; b) W. M. Brown, P. Wang, S. J. Plimpton, A. N. Tharrington, *Comput. Phys. Commun.* **2011**, *182*, 898.

[28] B. R. Elling, W. R. Dichtel, *ACS Cent. Sci.* **2020**, *6*, 1488.

[29] Y. Ding, A. P. Sokolov, *Macromolecules* **2006**, *39*, 3322.

[30] H. H. Winter, *Polym. Eng. Sci.* **1987**, *27*, 1698.

[31] a) S. Samanta, S. Kim, T. Saito, A. P. Sokolov, *J. Phys. Chem. B* **2021**, *125*, 9389; b) M. Tress, K. Xing, S. Ge, P. Cao, T. Saito, A. Sokolov, *Eur. Phys. J. E* **2019**, *42*, 133.

[32] W. Zou, J. Dong, Y. Luo, Q. Zhao, T. Xie, *Adv. Mater.* **2017**, *29*, 1606100.

[33] a) D. Qi, K. Zhang, G. Tian, B. Jiang, Y. Huang, *Adv. Mater.* **2021**, *33*, 2003155; b) J. Deng, X. Kuang, R. Liu, W. Ding, A. C. Wang, Y.-C. Lai, K. Dong, Z. Wen, Y. Wang, L. Wang, H. J. Qi, T. Zhang, Z. L. Wang, *Adv. Mater.* **2018**, *30*, 1705918; c) Q. Zhang, S. Niu, L. Wang, J. Lopez, S. Chen, Y. Cai, R. Du, Y. Liu, J.-C. Lai, L. Liu, C.-H. Li, X. Yan, C. Liu, J. B. H. Tok, X. Jia, Z. Bao, *Adv. Mater.* **2018**, *30*, 1801435.

[34] X. Chen, X. Gao, A. Nomoto, K. Shi, M. Lin, H. Hu, Y. Gu, Y. Zhu, Z. Wu, X. Chen, X. Wang, B. Qi, S. Zhou, H. Ding, S. Xu, *Nano Res.* **2021**, *14*, 3248.

Manuscript received: July 31, 2023
Accepted manuscript online: October 2, 2023
Version of record online: October 17, 2023